Activation of Rho through a cross-link with polyamines catalyzed by *Bordetella* dermonecrotizing toxin

Minako Masuda, Lazaro Betancourt[1], Takeshi Matsuzawa, Takashige Kashimoto, Toshifumi Takao[1], Yasutsugu Shimonishi[1] and Yasuhiko Horiguchi[2]

Project Research for Molecular Bacteriology, Research Institute for Microbial Diseases, Osaka University, Yamada-oka 3-1 and [1]Division of Organic Chemistry, Institute for Protein Research, Osaka University, Yamada-oka 3-2, Suita, Osaka 565-0871, Japan

[2]Corresponding author
e-mail: horiguti@biken.osaka-u.ac.jp

The small GTPase Rho, which regulates a variety of cell functions, also serves as a specific substrate for bacterial toxins. Here we demonstrate that *Bordetella* dermonecrotizing toxin (DNT) catalyzes cross-linking of Rho with ubiquitous polyamines such as putrescine, spermidine and spermine. Mass spectrometric analyses revealed that the cross-link occurred at Gln63, which had been reported to be deamidated by DNT in the absence of polyamines. Rac1 and Cdc42, other members of the Rho family GTPases, were also polyaminated by DNT. The polyamination, like the deamidation, markedly reduced the GTPase activity of Rho without affecting its GTP-binding activity, indicating that polyaminated Rho behaves as a constitutively active analog. Moreover, polyamine-linked Rho, even in the GDP-bound form, associated more effectively with its effector ROCK than deamidated Rho in the GTP-bound form and, when microinjected into cells, induced the anomalous formation of stress fibers indistinguishable from those seen in DNT-treated cells. The results imply that the polyamine-linked Rho, transducing signals to downstream ROCK in a novel GTP-independent manner, plays an important role in DNT cell toxicity.

Keywords: *Bordetella* dermonecrotizing toxin/polyamine/Rho/transglutaminase

Introduction

The Rho family of GTPases regulate various cellular processes including cytoskeletal organization (Hall, 1998), cell motility (Takaishi *et al*., 1994), cytokinesis (Madaule *et al*., 1998), gene expression (Hill *et al*., 1995) and cell cycle progression (Yamamoto *et al*., 1993; Olson *et al*., 1995). They function as molecular switches shuttling between inactive GDP-bound and active GTP-bound forms. The GTPases, which are in the GDP-bound form in resting cells, exchange GDP for GTP when stimuli arrive, transduce signals to downstream effector proteins and thereafter return to the inactive GDP-bound form by hydrolyzing the bound GTP. Many accessory factors modulate these processes: the GDP–GTP exchange reac-

tion is inhibited by GDP dissociation inhibitor (GDI) but accelerated by GDP/GTP exchange factor. The intrinsic GTPase activity is activated by GTPase-activating protein (GAP). The Rho-dependent signals are possibly diverged from the effector proteins and thereby involved in a variety of cellular processes. For instance, ROCK (or ROK/Rho-kinase) and mDia, the effector proteins, cooperatively mediate the signal from Rho to stress fiber formation (Watanabe *et al*., 1999). Citron kinase has been reported to be involved in cytokinesis (Madaule *et al*., 1998). ROCK and the myosin-binding subunit of myosin phosphatase participate in regulating smooth muscle contraction (Kimura *et al*., 1996; Kureishi *et al*., 1997). In addition, many proteins such as rhotekin (Reid *et al*., 1996), rhophilin (Watanabe *et al*., 1996) and protein kinase N (Amano *et al*., 1996; Watanabe *et al*., 1996) have been identified as Rho effectors, although their functions still remain unknown.

These small GTPases also serve as substrates for several groups of bacterial protein toxin (Aktories, 1997). C3 exoenzyme from *Clostridium botulinum*, C3-like toxins from *Clostridium limosum* and *Bacillus cereus*, and epidermal cell differentiation inhibitor from *Staphylococcus aureus* constitute the largest family of ADP ribosyltransferases, which transfer the ADP-ribose moiety of NAD to Asn41 of Rho and consequently inhibit Rho function. *Pseudomonas aeruginosa* exotoxin S ADP-ribosylates Ras and several other GTPases (Coburn, 1992). Another family of toxins modifying the GTPases is glycosyltransferases (von Eichel-Streiber *et al*., 1996). *Clostridium difficile* toxin A and B and hemorrhagic toxin and lethal toxin from *Clostridium sordelli* transfer glucose from UDP-glucose to threonine in the effector domain of Rho family proteins. *Clostridium novyi* α-toxin transfers *N*-acetyl glucosamine from UDP-*N*-acetyl glucosamine to the same site of Rho proteins. These toxins are considered to affect host cells through modification of the GTPases. They have also provided insight into the functions of the GTPases when used as specific inhibitors.

We have demonstrated recently that *Bordetella* dermonecrotizing toxin (DNT) produced by bacteria belonging to the genus *Bordetella* deamidates Gln63 of Rho and the corresponding Gln61 of Rac1 and Cdc42, and converts them into glutamic acid (Horiguchi *et al*., 1997). This modification eliminates their GTPase activity and renders the GTPases constitutively active. The treatment of cultured cells with DNT results in massive formation of actin stress fibers and focal adhesions, which are indistinguishable from those seen in cells microinjected with RhoA[Val14], a well-known active mutant of RhoA. These results indicate that the deamidated Rho mediates the effects of DNT on the cells. In fact, we confirmed that transfection of the RhoA[Glu63] gene, a mutant equivalent to deamidated Rho, conferred the massive formation of stress fibers

on the cells. Cytotoxic necrotizing factors from some pathogenic strains of *Escherichia coli* have been reported to have a similar action (Flatau *et al.*, 1997; Schmidt *et al.*, 1997). Deamidated Rho was found to move more slowly than intact Rho on SDS–PAGE and was detected by antibody (anti-63E) specific to the deamidated GTPases of the Rho family (Flatau *et al.*, 1997; Horiguchi *et al.*, 1997; Schmidt *et al.*, 1997). However, we have found that most of the Rho in DNT-treated cells showed a downward shift in addition to the upward shift in SDS–PAGE, which has not been observed in cells treated with cytotoxic necrotizing factors. Anti-63E recognized the upward- but not the downward-shifted Rho. These facts imply that DNT intracellularly catalyzes a modification of Rho distinct from the deamidation. In this study, we attempted to identify the nature of this modification and to elucidate the mechanism by which the modified Rho up-regulates the formation of actin stress fibers. It was revealed that DNT catalyzes a cross-link between Gln63 of Rho and ubiquitous polyamines such as putrescine, spermidine and spermine. The polyamination, like the deamidation, reduced both the intrinsic and GAP-stimulated GTPase activities of Rho without affecting the GTP-binding activity. Furthermore, the polyaminated Rho interacted with downstream ROCK in a GTP-independent manner and induced the formation of actin stress fibers when microinjected into cells. Taken together with our previous data, these results suggest that DNT exerts its toxic effects by activating Rho in multiple ways through deamidation and polyamination. Despite interacting effectively with ROCK, the polyaminated Rho stimulated ROCK kinase activity at only the same or a slightly weaker magnitude than intact Rho. These findings also suggest that the signal transduction from Rho to ROCK is dependent on the association with ROCK but not on the stimulation of its kinase activity.

Results

Cross-linking of the Rho GTPases with polyamines by DNT

We have reported that recombinant Rho was deamidated by *in vitro* treatment with DNT, which resulted in an upward shift of the electrophoretical mobility of Rho (Horiguchi *et al.*, 1995, 1997) (Figure 1B, lane 2). In contrast, intracellular Rho was split into three different bands on SDS–PAGE after treatment of whole cells or the cell lysates with the toxin (Figure 1A, lanes 2 and 4); the upper and intermediate bands turned out to be the deamidated and intact Rho, respectively, as reported previously (Horiguchi *et al.*, 1997). The nature of the lower band remains unknown. To analyze the type of modification yielding the downward-shifted Rho, we tried to obtain a large amount of modified Rho by the co-expression method (Kashimoto *et al.*, 1999), in which FLAG-tagged RhoA was co-expressed with DNT in *E.coli* and underwent modification intrabacterially. As shown in Figure 2, the intrabacterial modification generated the downward-shifted Rho similar to that in the mammalian cells. The modified FLAG-RhoA was purified by anti-FLAG affinity chromatography and subjected to reversed-phase HPLC. The proteins that differed in retention time were eluted and measured by Matrix-assisted laser desorption ioniza-
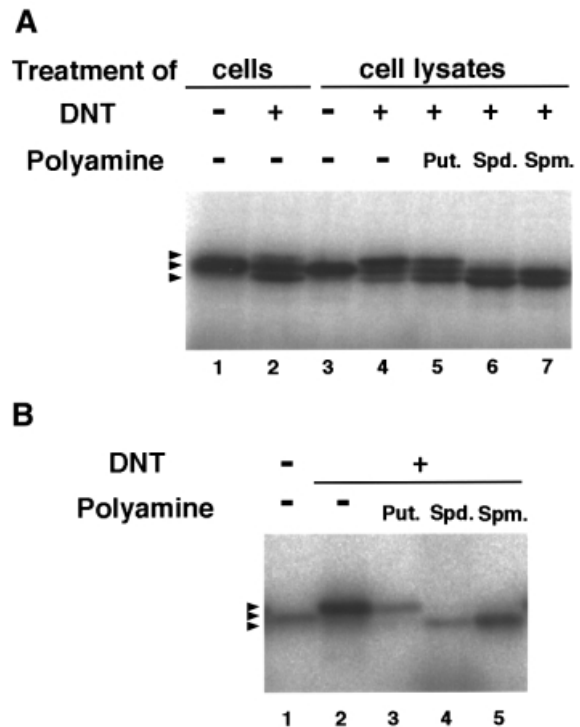

Fig. 1. Mobility shifts of Rho on SDS–PAGE after treatment with DNT. (**A**) Lanes 1 and 2, after overnight incubation with (lane 2) or without (lane 1) 5 ng/ml DNT, Swiss 3T3 cells were scraped and disrupted by sonication; lanes 3–7, after disruption, the cell lysates were treated with 10 µg/ml DNT in the absence (lane 4) or presence of 250 µM putrescine (lane 5), spermidine (lane 6) or spermine (lane 7). Lane 3, control cell lysate. (**B**) The recombinant RhoA was treated with DNT at a molar ratio of 20:1 in the presence or absence of 250 µM polyamines. Rho proteins were visualized by autoradiography after [^{32}P]ADP-ribosylation by C3 exoenzyme and SDS–PAGE. The arrowheads indicate the positions of Rho with different electrophoretical mobility.

tion time-of-flight mass spectrometry (MALDI-TOFMS) giving MH^+ ions at *m/z* 22 976.4, 23 105.9, 23 049.5 and 22 979.1, which agreed well with the theoretical molecular masses of RhoA (22 977.1), RhoA cross-linked with spermidine (23 106.3) and putrescine (23 049.2), and the intact or deamidated RhoA (22 978.1), respectively (the intact and deamidated proteins could not be discriminated from each other under the present conditions). The modified sites for each protein were located in the peptide Asp59–Arg68 of RhoA by peptide mapping with reversed-phase HPLC and MALDI-TOFMS. These peptides were subjected to post-source decay (PSD) analysis on MALDI-TOFMS. The backbone-fragmented ion species (y'', *b*, *z*, etc.) revealed a modification at Gln63, the residue deamidated with DNT as reported previously (Horiguchi *et al.*, 1997). These results imply that DNT catalyzes a cross-link of Rho with the ubiquitous polyamines putrescine and spermidine, and the polyamination results in the downward shift of Rho on SDS–PAGE. To examine this, we treated the lysates of cells and recombinant RhoA with DNT in the presence of the polyamines putrescine, spermidine and spermine, all of which are known to be abundant in mammalian cells. The cell lysates treated with DNT in the presence of the polyamines clearly showed a downward-shifted Rho (Figure 1A, lanes 5–7). The effect was less apparent for putrescine. The
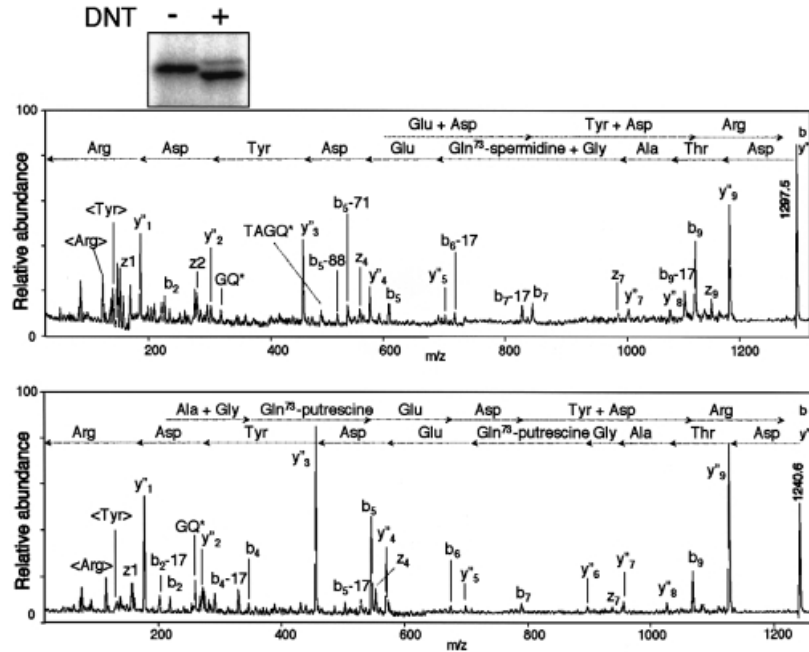
Fig. 2. PSD analysis of the modified peptides of RhoA (Asp59–Arg68). The upper and lower panels show the spectra of the peptides derived from RhoA cross-linked with spermidine (m/z 23 105.9) and putrescine (m/z 23 049.5), respectively. The arrows ($\leftarrow$ and $\rightarrow$) show the sequences from the N- and C-termini, based on y''_m and b_l ions, respectively, where m and l denote the arbitrary positions counted from the C- and N-termini, which were produced by cleavage of peptide bonds during mass measurement. <Arg> and <Tyr> in the low mass region denote immonium ions. The nomenclature of these ions is in accordance with previous work (Johnson *et al.*, 1987). Gln73 in this figure indicates Gln63 of native RhoA, because the FLAG-RhoA has an N-terminal 10 amino acid extension of the FLAG peptide. Inset, mobility shifts on SDS–PAGE of FLAG-RhoA expressed with (+) or without (–) DNT in *E.coli*. FLAG-RhoA was purified, [^{32}P]ADP-ribosylated with C3 exoenzyme and subjected to SDS–PAGE. Note that intrabacterially modified FLAG-RhoA shows mobility shifts similar to those of Rho in the DNT-treated cells (see Figure 1A, lane 2).

recombinant RhoA also showed the downward shift when treated with DNT in the presence of spermidine and spermine (Figure 1B, lanes 4 and 5). The downward-shifted Rho was barely observed in the presence of putrescine (Figure 1B, lane 3). From these results, we consider that DNT is a transglutaminase, catalyzing a cross-link between Gln63 of Rho and the polyamines, and that the polyamination causes the downward shift of Rho on SDS–PAGE.

We next examined the members of the Rho family for sensitivity to DNT. As judged by the incorporation of ^{14}C-labeled polyamines, RhoA, Rac1 and Cdc42, but not Ha-Ras, were found to be susceptible to DNT (Figure 3A). RhoA and Rac1 were better substrates than Cdc42. Putrescine was incorporated into the GTPases less effectively than spermidine and spermine. No polyamines were incorporated into RhoA^{Glu63}, the mutant equivalent to the deamidated Rho in which Glu is substituted for Gln63, indicating that, once deamidated, Rho does not undergo polyamination. To elucidate whether DNT causes poly-amination *in vivo*, we treated with DNT, C3H10T1/2 cells in which spermidine and spermine had been radiolabeled metabolically by [^{14}C]putrescine. At least three kinds of cellular proteins were found to be radiolabeled by treatment with DNT (Figure 3B). The apparent molecular masses of the labeled proteins ranged from 21 to 25 kDa, which correspond to the values for the small GTPases. Furthermore, the immunoprecipitation assay revealed that FLAG-RhoA expressed in the cells was ^{14}C-polyaminated after treatment of cells with DNT. The polyaminated FLAG-RhoA was not detected in the untreated cells by immunoprecipitation assay (data not shown). In contrast
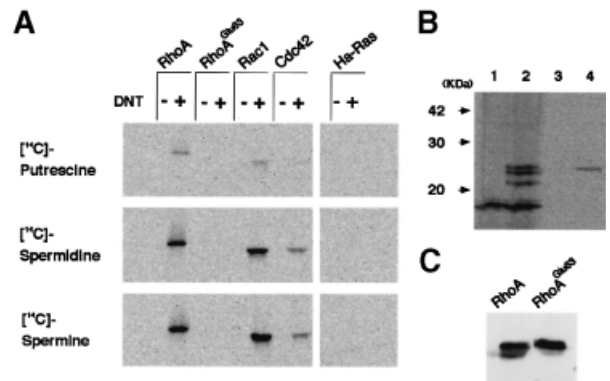

Fig. 3. Incorporation of [^{14}C]polyamines into GTPases and cellular proteins by the action of DNT. (**A**) The recombinant GTPases were treated with DNT at a molar ratio of 20:1 in the presence of 250 μM [^{14}C]putrescine, [^{14}C]spermidine or [^{14}C]spermine (7.8 GBq/mmol) as described in Materials and methods. The radiolabeled proteins were detected by autoradiography. (**B**) Lanes 1 and 2, C3H10T1/2 cells were pre-loaded with [^{14}C]putrescine and then incubated with (lane 2) or without (lane 1) 5 ng/ml DNT as described in Materials and methods. Cells were washed, lysed in SDS sample buffer and subjected to SDS–PAGE. Lanes 3 and 4, C3H10T1/2 cells expressing FLAG-RhoA^{Glu63} (lane 3) or FLAG-RhoA (lane 4) were pre-loaded with [^{14}C]putrescine and treated with DNT. After lysing the cells, FLAG-tagged proteins were immunoprecipitated and subjected to SDS–PAGE. The radiolabeled proteins were detected by autoradiography. (**C**) In order to check the expression level, the same quantities of the immunoprecipitates were subjected to SDS–PAGE and immunoblot analysis with anti-RhoA antibody.

to FLAG-RhoA, expressed FLAG-RhoA^{Glu63} was not polyaminated intracellularly by DNT (Figure 3B, lane 3). This result agrees with that of the *in vitro* experiment
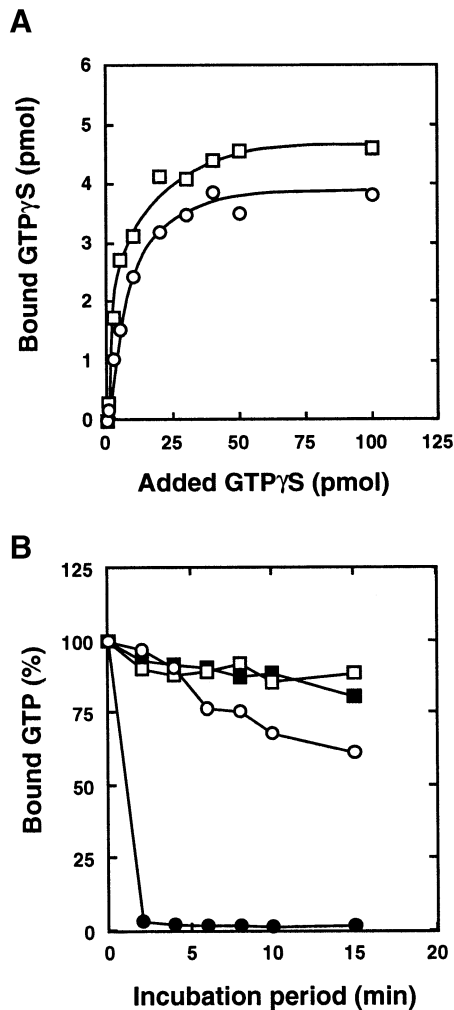
523

A

B

Fig. 4. GTPγS binding and GTPase activities of RhoA polyaminated by DNT. The recombinant RhoA (5 μM) was treated with DNT (50 nM) in the presence of 250 μM spermidine and examined for GTPγS binding (**A**) and GTPase activities (**B**). (○), Control RhoA; (□), spermidine-linked RhoA. In (B), GAP-stimulated GTPase activities of control RhoA (●) and spermidine-linked RhoA (■) were also determined. Three independent experiments were performed and representative results are shown.

with recombinant FLAG-RhoA[Glu63]. We attempted to determine whether Rac1 and Cdc42 are also polyaminated *in vivo*. However, the results of the immunoprecipitation assay were not stably reproduced, unlike the case of Rho, and therefore this issue remains inconclusive.

Effect of the polyamination on the nucleotide binding and GTPase activities of RhoA

We examined the effects of the polyamination on the GTPγS binding and GTPase activities of Rho. As shown in Figure 4A, the binding activity was not altered although the K_d value for polyaminated Rho (57.9 ± 7.3 nM, mean ± SE of data from three independent experiments) was significantly lower than that for intact Rho (101.9 ± 10.6 nM, $P < 0.05$). In contrast, the GTPase activity was obviously influenced by polyamination (Figure 4B). Both intrinsic and GAP-stimulated GTPase activities were decreased or abolished by the polyamination.

A GTP-independent induction of stress fiber formation by microinjection with polyaminated RhoA

Microinjection of polyaminated RhoA at 200 μg/ml into MC3T3-E1 cells apparently caused the formation of actin stress fibers within 1 h, indicating that the polyaminated Rho mediates DNT-induced actin fiber formation (Figure 5E and F). This effect was diminished by incubating the cells with Y27632, an inhibitor specific to ROCK (Uehata *et al.*, 1997) (Figure 5G and H). Neither intact RhoA nor the deamidated RhoA stimulated stress fiber formation when microinjected at 400 μg/ml (Figure 5A–D). It was reported that microinjection of normal Rho at a higher concentration caused the morphological changes (Paterson *et al.*, 1990). Similarly, microinjection of our preparations of RhoA and the deamidated RhoA induced the reorganization of actin stress fibers at 1.5 and 0.8 mg/ml, respectively (data not shown). When preloaded with GTPγS, RhoA and the deamidated RhoA at 400 μg/ml were found to induce stress fiber formation (Figure 5I–L).

Effects of polyamination on the interaction between RhoA and ROCK

Among several effector proteins for Rho identified to date, ROCK proteins are considered to play a key role in the rearrangement of stress fibers and focal adhesions (Leung *et al.*, 1996; Amano *et al.*, 1997; Ishizaki *et al.*, 1997), both of which occur in the DNT-treated cells. Thus, we examined the interaction of polyaminated RhoA with ROCK-I. The fragment ROCK-I Gln918–Phe1048 (ROCK-RB), which includes the Rho-binding domain (Fujisawa *et al.*, 1996; Leung *et al.*, 1996; Matsui *et al.*, 1996), was expressed as a GST fusion protein, purified and used as an immobilized ligand for the BIAcore system, which enables a real time evaluation of the interaction between RhoA and ROCK-RB. Consistent with the results of others (Leung *et al.*, 1995; Ishizaki *et al.*, 1996; Matsui *et al.*, 1996), RhoA bound to ROCK-RB in a GTP-dependent fashion (Figure 6A). The deamidated RhoA in the GTPγS-bound form was found to bind to ROCK-RB ~2-fold more than GTPγS-RhoA as judged by response in resonance units (RUs). Even in the GDP-bound form, the deamidated RhoA showed binding equivalent to that for GTPγS-RhoA (Figure 6B). Surprisingly, the polyaminated RhoA bound to ROCK-RB in a GTP-independent manner with a magnitude >3 times that of GTPγS-RhoA (Figure 6C).

We then investigated the kinase activities of ROCK in the presence of deamidated or polyaminated RhoA (Figure 7). For this experiment, ROCK-II purified from bovine brain was used because full-length ROCK-I could not be obtained from *E.coli* expression systems. Consistent with previous results (Ishizaki *et al.*, 1996; Leung *et al.*, 1996; Matsui *et al.*, 1996), GTPγS-RhoA stimulated the kinase activity up to ~2-fold more than GDP-RhoA. RhoA[Glu63] in the GTPγS-bound form potentiated the kinase activity >3 times more than in the GDP-bound form. Unexpectedly, the kinase activities in the presence of the polyaminated Rho were almost equivalent to or slightly lower than those in the presence of RhoA or RhoA[Glu63]. The polyaminated RhoA in the GTPγS form significantly
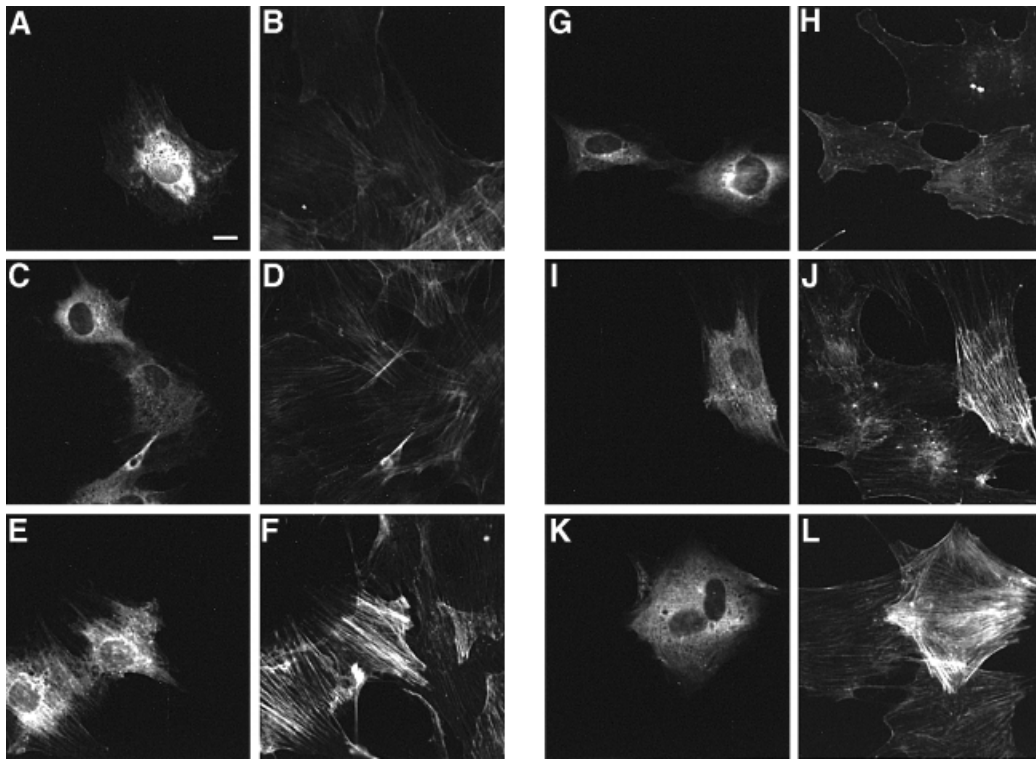
Fig. 5. Formation of actin stress fibers in MC3T3-E1 cells microinjected with RhoA. Microinjected cells were distinguished by staining with Alexa 488–anti-rabbit IgG (**A**, **C**, **E**, **G**, **I** and **K**) and the actin cytoskeleton was visualized by staining with Alexa 568–phalloidin (**B**, **D**, **F**, **H**, **J** and **L**). Cells were microinjected with 400 µg/ml control RhoA (A, B, I and J), 400 µg/ml RhoA treated with DNT in the absence of spermidine (C, D, K and L) or 200 µg/ml RhoA treated with DNT in the presence of spermidine (E–H). (G and H) Cells were incubated in the presence of 30 µM Y27632 for 1 h after microinjection. (I–L) The GTPases were pre-loaded with 120 µM GTPγS before microinjection. Bar, 10 µm.

but only slightly stimulated the kinase activities, compared with the GDP form.

Susceptibilities of Rho in various states to DNT

To obtain further insight into the intracellular action of DNT, we investigated the time course of the polyamination and deamidation. The polyamination of Rho preceded the deamidation, in accordance with previous observations (Horiguchi *et al.*, 1995), when the cells were treated with DNT; intracellular Rho was polyaminated 2 h after addition of DNT and its level increased until 6 h, as judged by the intensity of the lower band on SDS–PAGE (Figure 8A). The deamidation was detectable at 6 h. Eventually, the polyaminated and deamidated Rho reached 40 and 25% of total Rho, respectively. In resting cells, Rho is present in the GDP-bound form associated with GDI. When stimuli arrive, Rho is released from GDI, which makes the nucleotide exchange possible. Therefore, we examined whether GDI or guanine nucleotide influence the suscepti-bility of Rho to DNT. The recombinant RhoA was not deamidated by DNT in the presence of GTPγS (Figure 8B). Similarly, the modifications of Rho in the cell lysate were also inhibited with increasing amounts of GTPγS but not GDP (Figure 8C). These results indicate that the GDP-bound but not the GTP-bound form of Rho was sensitive to DNT. GDI also inhibited the modifications of Rho in the cell lysate, indicating that Rho associated with GDI was insensitive to DNT (Figure 8D).

Discussion

Here, we demonstrated that DNT is essentially a transglut-aminase, and exerts a toxic effect by catalyzing a cross-

link between Gln63 of Rho and ubiquitous polyamines. The transglutaminases are known to constitute a large protein family, and to be widely distributed in the tissues and body fluid of vertebrates (Folk, 1980; Aeschilimann and Paulsson, 1994). Some transglutaminases from bac-terial sources have also been reported (Kanaji *et al.*, 1993; Schmidt *et al.*, 1998). Although a number of reports have demonstrated that the polyamines are covalently linked to protein-bound Gln, they have not provided any information as to the biological significance of these covalent reactions (Folk *et al.*, 1980; Chen, 1984; Beninati and Folk, 1988; Cordella-Miele *et al.*, 1993). To our knowledge, this is the first report showing that the polyamination alters the function of the cellular protein and exerts biological effects on living cells. We demonstrated that DNT utilized putrescine, spermidine and spermine as co-substrates and catalyzed a cross-link with members of the Rho GTPase family *in vitro*. We consider that spermidine- or spermine-linked GTPases are crucial in eliciting the effects of DNT on mammalian cells, although putrescine was less effective as a co-substrate *in vitro* and, moreover, its intracellular concentration is known to be lower than that of other polyamines (Beppu *et al.*, 1995). In contrast, putrescine is abundant in prokaryotic cells (Kashiwagi and Igarashi, 1988), which is probably the reason why the putrescine-linked RhoA was recovered from *E.coli* by the co-expression method in this study.

The reorganization of stress fibers and focal adhesions, which are mediated by ROCK family proteins, is one of the most apparent phenomena observed in mammalian cells due to the toxic effects of DNT. In this study, we showed that the polyaminated RhoA, even in the GDP-
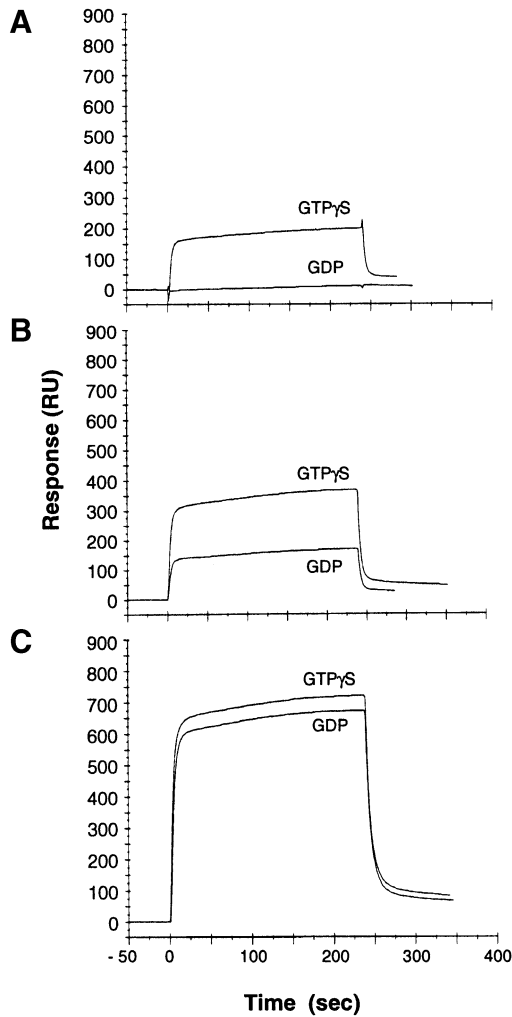
Fig. 6. Binding of RhoA to ROCK-RB. FLAG-RhoA (**A**), FLAG-RhoA[Glu63] (**B**) and polyaminated FLAG-RhoA (**C**) were examined for binding to ROCK-RB. The experiments were carried out five times with different concentrations of RhoA samples. The results with 6 μM RhoA are shown.
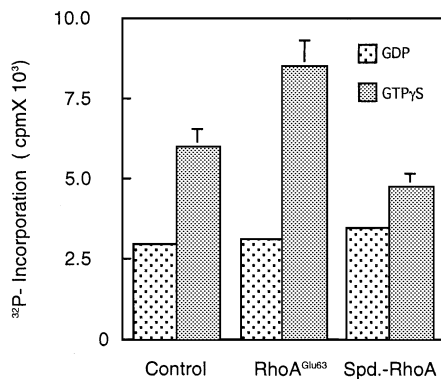

Fig. 7. Kinase activity of ROCK in the presence of the modified RhoA. The kinase activity of ROCK-II was examined in the presence of intact RhoA, RhoA[Glu63] or spermidine-linked RhoA in the GDP- or GTPγS-bound form. The experiments were performed independently three times and representative data are shown. Each bar shows the mean ± SD (n = 3). SD values in the experiments with GDP–GTPases have been omitted because they are too small to depict.
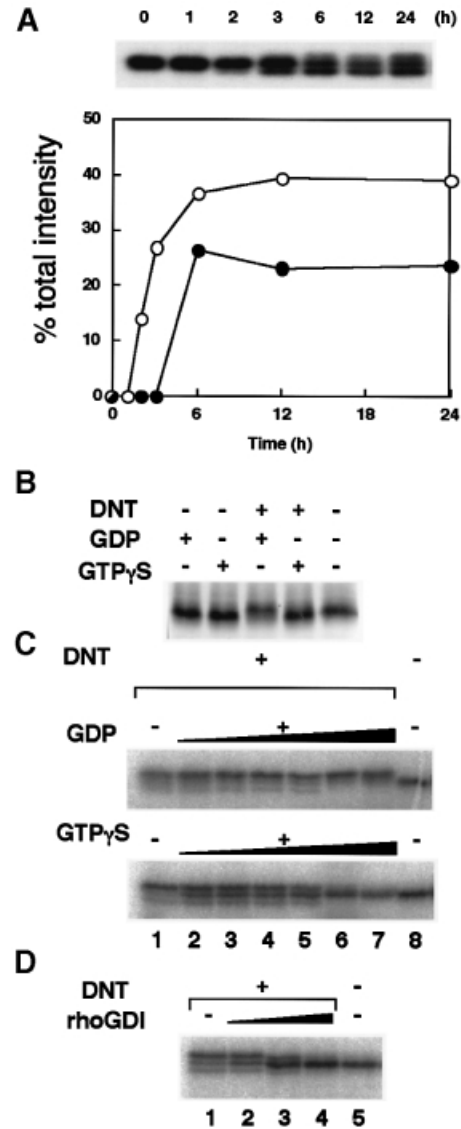

Fig. 8. Modification of Rho by DNT. (**A**) Time course of Rho modification in DNT-treated cells. MC3T3-E1 cells were treated with 5 ng/ml DNT under serum-starved conditions. The cells were disrupted by sonication and Rho was labeled specifically with [^{32}P]ADP-ribose by the C3 exoenzyme and then subjected to SDS–PAGE and autoradiography. Upper panel, patterns of mobility shifts of Rho on SDS–PAGE. Lower panel, radioactivities of the polyaminated and downward-shifted Rho (○), and the deamidated and upward-shifted Rho (●) relative to total radioactivity. (B and C) Guanine nucleotide dependency of the modification of recombinant RhoA (**B**) and Rho (**C**) in cell lysates by DNT. The recombinant RhoA (3 μM) was treated with DNT (0.15 μM) in the absence or presence of 10 μM GDP or GTPγS. SDS–PAGE sample buffer was added to stop the reaction and the sample was subjected to SDS–PAGE. The RhoA samples on the gel were detected directly by silver staining. (C) The lysates of Swiss 3T3 cells were pre-loaded with GTPγS or GDP at 30°C for 30 min, treated with DNT, and examined for mobility shifts on SDS–PAGE. Concentrations of guanine nucleotides in the reaction mixture were 0.05, 0.25, 0.5, 1, 10 and 20 mM from lane 2 to lane 7, respectively. (**D**) The effect of GDI on DNT-induced modification of Rho. The lysates of Swiss 3T3 cells were treated with DNT in the presence of GDI. GDI concentrations in the reaction mixture were 12.5, 65 and 250 nM from lane 2 to lane 4, respectively.

bound form, was able to interact with ROCK and induced stress fiber formations, without particularly stimulating the ROCK kinase activity. The kinase activity of ROCK
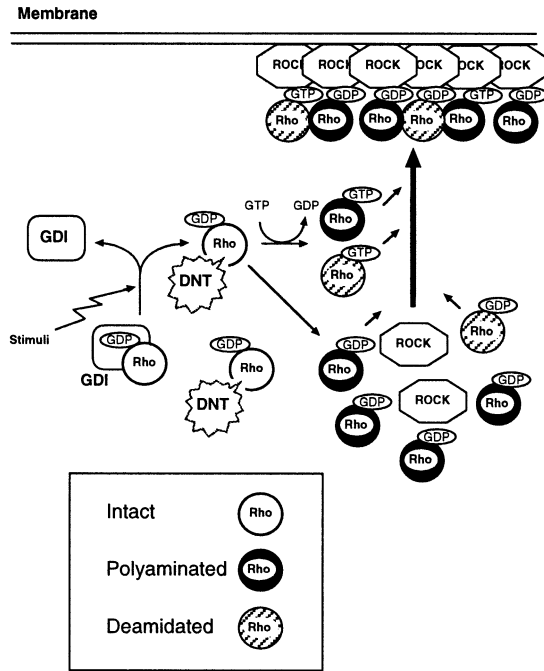
Fig. 9. A model depicting the intracellular action of DNT and functions of the modified Rho.

was undoubtedly essential because kinase-defective mutants of ROCK have been shown to inhibit the formation of stress fibers induced by lysophosphatidic acid (LPA) and a constitutively active mutant of Rho (Leung *et al.*, 1996; Amano *et al.*, 1997; Ishizaki *et al.*, 1997). This is also the case for the stress fiber formation induced by the polyaminated Rho: Y27632, a specific inhibitor of ROCK, inhibited stress fiber formation in cells microinjected with polyaminated Rho (Figure 5) or treated with DNT (data not shown). However, our results indicated that the signal transduction from Rho to ROCK is dependent on their molecular interaction and not on the increase in ROCK kinase activity. This raises the question of how the molecular interaction triggers the signal transduction. One possible explanation is that Rho changes the conformation of ROCK and thereby makes it possible to mediate downstream events. Similar examples of this hypothesis have been shown for N-WASP with Cdc42 (Miki *et al.*, 1998) and mDia1 with Rho (Watanabe *et al.*, 1999). mDia1, which is also essential for Rho-induced actin reorganization, forms intramolecular bonds between its N- and C-termini in the inactive form. It has been shown that this intramolecular association was disrupted upon the binding of GTP-Rho to the Rho-binding domain in the N-terminus, and exposed the C-terminal unit responsible for actin fiber formation. A similar conformational change may occur in ROCK, although there has been no evidence for the intramolecular binding of ROCK. Alternatively, the bound Rho may recruit ROCK to a site where it exerts its action. This idea is supported by the previous observation that the intracellular distribution of ROCK was changed by overexpression of wild-type or an active mutant of RhoA (Leung *et al.*, 1995; Sin *et al.*, 1998).

Figure 9 depicts a model of DNT action and interaction between ROCK and Rho modified by DNT on the basis of previous and the present data. DNT probably polyamin-

ates or deamidates GDP-Rho after GDI is liberated, or the bound GTP is hydrolyzed because GTP-Rho and GDP-Rho associated with GDI were not sensitive to DNT. The polyaminated Rho, which probably plays an important role in inducing stress fiber formation, because the increases in polyamination (Horiguchi *et al.*, 1995; this study) and cellular content of F-actin (Horiguchi *et al.*, 1995) show similar time courses after DNT treatment, interacts with the downstream ROCK in a nucleotide-independent manner. The deamidated Rho might contribute to this nucleotide-independent activation of ROCK because it also associated moderately with ROCK even in the GDP-bound form. The deamidated and polyaminated Rho retained the ability to bind GTP. Therefore, part of the modified Rho exchanges GDP for GTP and becomes constitutively active, because the GTP-hydrolyzing activity of Rho is abolished by the deamidation and polyamination. The time course of the mobility shifts of Rho in the DNT-treated cells implies that DNT first causes the polyamination. The deamidation was observed later than the polyamination; it may occur after the intracellular polyamines are consumed or DNT may catalyze the polyamination preferentially. The latter explanation is more likely because spermidine and spermine have been reported to be present at the millimolar level in mammalian cells (Janne *et al.*, 1978; Beppu *et al.*, 1995) and therefore must barely be consumed by the polyamination of Rho. Furthermore, we found that DNT caused the polyamination on RhoA in the presence of spermidine at a concentration as low as 100 μM (data not shown). The modified Rho may eventually function as a constitutively active analog in multiple ways and induce the anomalous formations of actin stress fibers and focal adhesions. Whether all the polyaminated GTPases including Rac and Cdc42 behave universally as constitutively active analogs toward every effector protein is an important question. Because the different regions of GTPases have been shown to participate in the molecular interaction with different effectors (Fujisawa *et al.*, 1998; Zong *et al.*, 1999), it is possible that the polyamination of GTPases activates only the restricted signaling pathway in which downstream effectors sensitive to the polyaminated GTPase are implicated. We have demonstrated that, in addition to cytoskeletal reorganization, DNT has a variety of biological activities, including stimulation of protein and DNA synthesis, inhibition of cytokinesis and inhibition of the expression of differentiated phenotypes in osteoblastic MC3T3-E1 cells (Horiguchi *et al.*, 1991, 1993). These effects may result from the overall activation of the Rho family GTPases polyaminated or deamidated by DNT. Each GTPase has multiple effector proteins, which are common to some GTPases or specific to a particular one. Therefore, the effects of DNT on cell function appear to be complex. To understand better the molecular basis of DNT toxicity, it will be important to correlate the effects of DNT with the constitutive activation of each GTPase and the signaling pathway to the downstream effector proteins.

Materials and methods

Materials

DNT was purified from *Bordetella bronchiseptica* by the method previously reported (Horiguchi *et al.*, 1990). The recombinant proteins

of RhoA, RhoA^{Glu63}, Rac1 and Cdc42 were obtained as described elsewhere (Horiguchi *et al.*, 1997). The expression vectors for mammalian cells, pMEPyori FLAG-RhoA and pMEPyori FLAG-RhoA^{Glu63}, were constructed as described in Horiguchi *et al.* (1997). GST-tagged Ha-Ras and RhoA were purified with a glutathione–Sepharose 4B (Amersham Pharmacia Biotech., Uppsala, Sweden) column from lysates of *E.coli* DH5α harboring pGEX2T-Ha-Ras and pGEX1T-RhoA provided by Dr Y.Takai, Osaka University Medical School, Osaka, Japan and Dr M.Sugai, Hiroshima University, Hiroshima, Japan, respectively. A catalytic fragment of p190GAP was provided by Dr R.A.Weinberg, The Whitehead Institute for Biomedical Research, Cambridge, MA. Rho GDI was provided by Dr Y.Takai. Y27632 was a gift from Yoshitomi Pharmaceutical Industries, Osaka, Japan. The Rho-binding domain of ROCK-I (ROCK-RB) was produced as an N-terminally GST-tagged protein as follows. A gene encoding the 918–1048 amino acid region of ROCK-I was amplified by PCR with primers (5′-CCGAATTCCCAA-GAAAGCAAGAAAGCTGCTTCAAG-3′, where the underlining indicates an *Eco*RI site, and 5′-ATGCGGCCGCGAATTTCTCTCTTT-CTTGGTTGAGTTC-3′, where the underlining indicates a *Not*I site) and pCMX-MycROCK as a template, which was provided by Dr S.Narumiya, Kyoto University Faculty of Medicine, Kyoto, Japan. The amplified DNA was subcloned into pBluescript SK⁻ (Stratagene, La Jolla, CA) treated with *Eco*RV and alkaline phosphatase. The ROCK-RB gene was excised from the plasmid obtained by treatment with *Eco*RI and *Not*I and was inserted into pGEX4T3 (Amersham Pharmacia) treated with the same enzymes. The GST fusion protein of ROCK-RB was purified from *E.coli* DH5α harboring this plasmid according to the manufacturer's manual. ROCK-II was purified from bovine brain by the method of Matsui *et al.* (1996). The purity of the kinase was confirmed by SDS–PAGE and immunoblotting with anti-ROCK-II antibody (C-20; Santa Cruz Biotechnology, Santa Cruz, CA). MC3T3-E1 and Swiss 3T3 and C3H10T1/2 cells were maintained in α-minimum essential medium (α-MEM) or in Dulbecco's modified Eagle's medium, respectively, supplemented with 10% fetal calf serum at 37°C under 5% CO_2 in air.

Intrabacterial modification of RhoA by DNT
RhoA was modified intrabacterially by DNT as described previously (Kashimoto *et al.*, 1999). DNT and FLAG-tagged RhoA were co-expressed in *E.coli* harboring pETDNTwt and pSTV29-FLAG-RhoA and allowed to react in bacterial cells during cultivation of the bacteria. The modified FLAG-RhoA was extracted from the bacterial cells and purified by affinity chromatography on an anti-FLAG M2–agarose gel (Sigma) according to the manufacturer's instructions. Unmodified FLAG-RhoA and FLAG-RhoA^{Glu63} were also recovered from *E.coli* carrying pET21d, a mock vector, and pSTV29-FLAG-RhoA or pSTV29-FLAG-RhoA^{Glu63}, respectively.

Structural analyses of modified Rho
The FLAG-RhoA samples were subjected to reversed-phase HPLC on a Develosil ODS-5C4-HG column (4.6 × 150 mm; Nomura Chemicals, Aichi, Japan). A linear gradient formed between solvent A [0.1% trifluoroacetic acid (TFA) in water] and solvent B (0.1% TFA in acetonitrile) was used for the separation. The proteins were eluted by increasing solvent B from 20 to 60% in 120 min at a flow rate of 1.0 ml/min and monitoring at both 214 and 280 nm. MALDI-TOFMS was performed with a Voyager Elite XL time-of-flight mass spectrometer equipped with a delayed extraction system (PE Biosystems, Framingham, MA) with flight paths of 4.2 and 6.5 m for the linear and reflectron mode, respectively. Solutions (1 μl) containing proteins (10 pmol) or peptides (1–5 pmol) were mixed with the matrix solution, the supernatant of a 50 or 33% acetonitrile solution saturated with α-cyano-4-hydroxy cinnamic acid or sinapinic acid, respectively, and then air dried on the flat surface of a stainless steel plate. The ions were generated by irradiating the sample area with the output of a nitrogen laser at a wavelength of 337 nm, and accelerated at a 20 or 25 kV potential in the ion source with a delay of 50 or 150 ns in the linear or PSD mode, respectively.

Treatment of cell lysates and GTPases with DNT
Swiss 3T3 cells were seeded into a 60 mm dish at a density of $1.5 × 10^4$ cells/cm² and incubated for 24 h. The cells were washed with phosphate-buffered saline (PBS), scraped with a rubber policeman in 10 mM sodium phosphate buffer pH 8.5, and homogenized by sonication. The homogenates were diluted with the same buffer to produce a protein concentration of 1 mg/ml. The homogenates (25 μg) were treated with 10 μg/ml DNT in 30 μl of the same buffer containing 5 mM dithiothreitol (DTT) for 2 h at 37°C. The recombinant GTPases were incubated with DNT in 20 mM Tris–HCl pH 7.5, 10 mM $MgCl_2$, 1 mM EDTA and 5 mM DTT at 37°C overnight.

Assay for in vivo polyamination
C3H10T1/2 cells were pre-loaded with 18.5 kBq/ml of [^{14}C]putrescine in the presence of 20 μM aminoguanizine at 37°C for 24 h as described before (Piacentini *et al.*, 1988), and then incubated with or without 5 ng/ml DNT for an additional 24 h. The cells were washed, lysed in the SDS sample buffer and subjected to SDS–PAGE. For immunoprecipitation, C3H10T1/2 cells were transfected with pMEPyori FLAG-RhoA or pMEPyori FLAG-RhoA^{Glu63} by the calcium phosphate method. After incubation for 2 days, the cells were pre-loaded with [^{14}C]putrescine and treated with DNT as described above. The cells were washed and lysed with cell lysis buffer (10 mM Tris–HCl pH 7.8, containing 1% NP-40, 0.15 M NaCl and 1 mM EDTA) at 4°C for 1 h. The lysates were incubated at 4°C for 2 h with anti-FLAG M2–agarose gel (Sigma) pre-washed with 5% skim milk and suspended in the cell lysis buffer. The agarose gel was washed with the cell lysis buffer and boiled in 2-fold concentrated SDS sample buffer, and the supernatant after centrifugation was subjected to SDS–PAGE. After electrophoresis, proteins linked to [^{14}C]polyamines were detected by autoradiography.

Microinjection
MC3T3-E1 cells were plated on coverslips at 7000 cells/cm² and incubated for 24 h as described above. The cells were washed with pre-warmed PBS, incubated further in serum-free α-MEM for 24 h and subjected to microinjection. The recombinant RhoA was treated with DNT at a molar ratio of 1000:1 in Dulbecco's PBS containing 0.1 mM GDP in the presence or absence of 1 mM spermidine at 37°C overnight. The RhoA samples were diluted appropriately and microinjected into the cells along with 1 mg/ml of rabbit IgG. Microinjection was performed with an Eppendorf micromanipulator (Eppendorf, Hamburg, Germany). The cells were incubated further for 1 h after microinjection, fixed with 3% paraformaldehyde in PBS for 10 min, washed three times with PBS and permeabilized with 0.5% Triton X-100 in PBS for 5 min. Alexa 568–phalloidin (Molecular Probes, Eugene, OR) and Alexa 488–goat anti-rabbit IgG (Molecular Probes) in PBS containing 10% fetal calf serum were overlaid on the cells at 2.5 U/ml and 4 μg/ml, respectively, and allowed to react at room temperature for 1 h. The cells were washed with PBS, mounted in PermaFluor™ aqueous mounting medium (Immunon, Pittsburgh, PA) and observed under a fluorescence microscope. Fluorescence micrographs were taken with a SPOT color digital camera (Diagnostic Instruments, Sterling Heights, MI) controlled by IP Lab software (Scanalytics, Fairfax, VA).

Assays of GTPγS binding and GTPase activities
The GTPγS binding activity of GTPases was determined by the method described elsewhere (Horiguchi *et al.*, 1997). GTPase activity was determined according to the method of Kikuchi *et al.* (1989) with a slight modification. The recombinant RhoA (200 pmol) was pre-incubated for 20 min at 30°C in 100 μl of 20 mM Tris–HCl pH 7.5 containing 5 mM $MgCl_2$, 10 mM EDTA, 5 mM DTT and 1 μM [γ-^{32}P]GTP (~9000 c.p.m./pmol). Reaction buffer (100 μl) containing 20 mM Tris–HCl pH 7.5, 25 mM $MgCl_2$, 4 mM GTP and 7.5 mM DTT was added with or without 30 μg/ml of the catalytic fragment of p190GAP to the pre-incubated mixture and incubated at 30°C. After various periods of incubation, 25 μl aliquots of the mixture were transferred into wells of a Multiscreen filter plate HA (Millipore) containing 100 μl of washing solution (20 mM Tris–HCl pH 8.0, 30 mM $MgCl_2$, 125 mM NaCl), and subjected to rapid filtration. The filter was washed five times with 200 μl of the washing solution and the radioactivity remaining on the filter membrane was measured with a scintillation counter.

Binding of RhoA to ROCK-RB
The binding of the intact and modified RhoA proteins to ROCK-RB was monitored with a BIAcore system (BIAcore, Uppsala, Sweden). The BIAcore system was operated at 25°C and at a constant flow of 5 μl/min in running buffer containing 20 mM Tris–HCl pH 7.5, 10 mM $MgCl_2$ and 1 mM EDTA. For immobilization of the GST-tagged ROCK-RB, a CM5 sensor chip was first coated with goat anti-GST antibody according to the manufacturer's instructions. The GST-tagged ROCK-RB (6 μg) was immobilized by injecting over the chip coated with anti-GST antibody. GST was also immobilized on another chip for control experiments. The efficiency of the immobilizations was confirmed by the increase in resonance units (RUs) to ~12 000. The FLAG-tagged RhoA proteins recovered by the co-expression method described above were dialyzed against 20 mM Tris–HCl pH 7.5 containing 5 mM $MgCl_2$,

pre-loaded with GDP or GTPγS at a 10-fold molar excess to the protein in the running buffer at 37°C for 2 h, and injected over the immobilized proteins. The polyaminated FLAG-tagged RhoA obtained from *E.coli* was found to consist of 32% putrescine-, 54% spermidine-linked RhoA and 14% deamidated RhoA, as calculated from a profile of reversed-phase HPLC (data not shown). Specific binding was estimated by subtracting the RUs of background binding in the control experiments from those of total binding in each experiment.

Protein kinase assay

GST-tagged RhoA was treated with DNT at a 1000:1 molar ratio in the presence or absence of 250 µM spermidine as described above, pre-loaded with GDP or GTPγS at a 10-fold molar excess to the GTPase in 20 mM Tris–HCl pH 8.0, 5 mM MgCl$_2$, 10 mM EDTA and 1 mM DTT at 30°C for 20 min, and used for the following kinase assay. The kinase reaction was carried out in 50 µl of Tris–HCl pH 8.0, 8 mM MgCl$_2$, 0.2% CHAPS, 10 µM [γ-^{32}P]ATP (~250 GBq/mmol), 2 µM GST–RhoA, 40 µM PKCα peptide as a substrate, and purified ROCK-II (10 ng). After incubation for 10 min at 30°C, the reaction mixture was spotted immediately onto Whatman p81 paper. The paper was washed five times in 300 ml of 75 mM phosphoric acid and dried in air. The radioactivity incorporated into the PKCα peptide on the paper was measured with a scintillation counter.

Other methods

The [^{32}P]ADP-ribosylation of Rho was achieved with C3 exoenzyme as described previously (Horiguchi *et al.*, 1995). Autoradiography was performed with an imaging plate (Fuji Film Co., Tokyo, Japan) and radioactive protein bands were detected using a Fuji BAS 1500 image analyzer (Fuji Film). For immunoblot analysis, samples were transferred to polyvinylidene difluoride membranes after SDS–PAGE. The membranes were probed with anti-RhoA antibody (119; Santa Cruz, CA) and alkaline phosphatase-conjugated anti-rabbit IgG. Immunoblots were revealed by CDP-Star reagent (Tropix, Bedford, MA).

Acknowledgements

References

Aeschilimann,D. and Paulsson,M. (1994) Transglutaminases: protein cross-linking enzymes in tissues and body fluids. *Thromb. Haemost.*, **71**, 402–415.

Aktories,K. (1997) Rho proteins: targets for bacterial toxins. *Trends Microbiol.*, **5**, 282–288.

Amano,M., Mukai,H., Ono,Y., Chihara,K., Matsui,T., Hamajima,Y., Okawa,K., Iwamatsu,A. and Kaibuchi,K. (1996) Identification of a putative target for Rho as the serine-threonine kinase protein kinase N. *Science*, **271**, 648–650.

Amano,M., Chihara,K., Kimura,K., Fukata,Y., Nakamura,N., Matsuura,Y. and Kaibuchi,K. (1997) Formation of actin stress fibers and focal adhesions enhanced by Rho-kinase. *Science*, **275**, 1308–1311.

Beninati,S. and Folk,J.E. (1988) Covalent polyamine–protein conjugates: analysis and distribution. *Adv. Exp. Med. Biol.*, **250**, 411–422.

Beppu,T., Shirahata,A., Takahashi,M., Hosoda,H. and Samejima,K. (1995) Specific depletion of spermidine and spermine in HTC cells treated with inhibitors of aminopropyltransferases. *J. Biochem.*, **117**, 339–345.

Chen,K.Y. (1984) Transglutaminase catalyzed incorporation of putrescine into surface proteins of mouse neuroblastoma cells. *Mol. Cell. Biochem.*, **58**, 91–97.

Coburn,J. (1992) *Pseudomonas aeruginosa* exoenzyme S. *Curr. Top. Microbiol. Immunol.*, **175**, 133–143.

Cordella-Miele,E., Miele,L., Beninati,S. and Mukherjee,A.B. (1993) Transglutaminase-catalyzed incorporation of polyamines into phospholipase A$_2$. *J. Biochem.*, **113**, 164–173.

Flatau,G., Lemichez,E., Gauthler,M., Chardin,P., Paris,S., Fiorentini,C. and Boquet,P. (1997) Toxin-induced activation of the G protein p21 Rho by deamidation of glutamine. *Nature*, **387**, 729–733.

Folk,J.E. (1980) Transglutaminase. *Annu. Rev. Biochem.*, **49**, 517–531.

Folk,J.E., Park,M.H., Chung,S.I., Schrode,J., Lester,E.P. and Cooper,H.L. (1980) Polyamines as physiological substrates for transglutaminases. *J. Biol. Chem.*, **255**, 3695–3700.

Fujisawa,K., Fujita,A., Ishizaki,T., Saito,Y. and Narumiya,S. (1996) Identification of the Rho-binding domain of p160^{ROCK}, a Rho-associated coiled-coil containing protein kinase. *J. Biol. Chem.*, **271**, 23022–23028.

Fujisawa,K., Madaule,P., Ishizaki,T., Watanabe,G., Bito,H., Saito,Y., Hall,A. and Narumiya,S. (1998) Different regions of Rho determine Rho-selective binding of different classes of Rho target molecules. *J. Biol. Chem.*, **273**, 18943–18949.

Hall,A. (1998) Rho GTPases and the actin cytoskeleton. *Science*, **279**, 509–515.

Hill,C.S., Wynne,J. and Treisman,R. (1995) The rho family GTPases rhoA, rac1 and cdc42Hs regulate transcriptional activation by SRF. *Cell*, **81**, 1159–1170.

Horiguchi,Y., Nakai,T. and Kume,K. (1990) Simplified procedure for purification of *Bordetella bronchiseptica* dermonecrotic toxin. *FEMS Microbiol. Lett.*, **66**, 39–43.

Horiguchi,Y., Nakai,T. and Kume,K. (1991) Effects of *Bordetella bronchiseptica* dermonecrotic toxin on the structure and function of osteoblastic clone MC3T3-E1 cells. *Infect. Immun.*, **59**, 1112–1116.

Horiguchi,Y., Sugimoto,N. and Matsuda,M. (1993) Stimulation of DNA synthesis in osteoblast-like MC3T3-E1 cells by *Bordetella bronchiseptica* dermonecrotic toxin. *Infect. Immun.*, **61**, 3611–3615.

Horiguchi,Y., Senda,T., Sugimoto,N., Katahira,J. and Matsuda,M. (1995) *Bordetella bronchiseptica* dermonecrotizing toxin stimulates assembly of actin fibers and focal adhesions by modifying the small GTP-binding protein rho. *J. Cell Sci.*, **108**, 3243–3251.

Horiguchi,Y., Inoue,N., Masuda,M., Kashimoto,T., Katahira,J., Sugimoto,N. and Matsuda,M. (1997) *Bordetella bronchiseptica* dermonecrotizing toxin induces reorganization of actin stress fibers through deamidation of Gln-63 of the GTP-binding protein Rho. *Proc. Natl Acad. Sci. USA*, **94**, 11623–11626.

Ishizaki,T. *et al.* (1996) The small GTP-binding protein Rho binds to and activates a 160 kDa Ser/Thr protein kinase homologous to myotonic dystrophy kinase. *EMBO J.*, **15**, 1885–1893.

Ishizaki,T., Naito,M., Fujiwara,K., Maekawa,M., Watanabe,N., Saito,Y. and Narumiya,S. (1997) p160ROCK, a Rho-associated coiled-coil forming protein kinase, works downstream of Rho and induces focal adhesions. *FEBS Lett.*, **404**, 118–124.

Janne,J., Poso,H. and Raina,A. (1978) Polyamines in rapid growth and cancer. *Biochim. Biophys. Acta*, **473**, 241–293.

Johnson,R.S., Martin,S.A., Biemann,K., Stults,J.T. and Watson,J.T. (1987) Novel fragmentation process of peptides by collision-induced decomposition in a tandem mass spectrometer: differentiation of leucine and isoleucine. *Anal. Chem.*, **59**, 2621–2625.

Kanaji,T., Ozaki,H., Takao,T., Kawajiri,H., Ide,H., Motoki,M. and Shimonishi,Y. (1993) Primary structure of microbial transglutaminase from *Streptoverticillium* sp. strain s-8112. *J. Biol. Chem.*, **268**, 11565–11572.

Kashimoto,T., Katahira,J., Cornejo,W.R., Masuda,M., Fukuoh,A., Matsuzawa,T., Ohnishi,T. and Horiguchi,Y. (1999) Identification of functional domains of *Bordetella* dermonecrotizing toxin. *Infect. Immun.*, **67**, 3727–3732.

Kashiwagi,K. and Igarashi,K. (1988) Adjustment of polyamine contents in *Escherichia coli*. *J. Bacteriol.*, **170**, 3131–3135.

Kikuchi,A., Sasaki,T., Araki,S., Hata,Y. and Takai,Y. (1989) Purification and characterization from bovine brain cytosol of two GTPase-activating proteins specific for smg p21, a GTP-binding protein having the same effector domain as c-*ras* p21s. *J. Biol. Chem.*, **264**, 9133–9136.

Kimura,K. *et al.* (1996) Regulation of myosin phosphatase by Rho and Rho-associated kinase (Rho-kinase). *Science*, **273**, 245–248.

Kureishi,Y., Kobayashi,S., Amano,M., Kimura,K., Kanaide,H., Nakano,T., Kaibuchi,K. and Ito,M. (1997) Rho-associated kinase directly induces smooth muscle contraction through myosin light chain phosphorylation. *J. Biol. Chem.*, **272**, 12257–12260.

Leung,T., Manser,E., Tan,L. and Lim,L. (1995) A novel serine/threonine kinase binding the Ras-related RhoA GTPase which translocates the kinase to peripheral membranes. *J. Biol. Chem.*, **270**, 29051–29054.

Leung,T., Chen,X., Manser,E. and Lim,L. (1996) The p160 RhoA-binding kinase ROKα is a member of a kinase family and is involved in the reorganization of the cytoskeleton. *Mol. Cell. Biol.*, **16**, 5313–5327.

Madaule,P., Eda,M., Watanabe,N., Fujisawa,K., Matsuoka,T., Bito,H., Ishizaki,T. and Narumiya,S. (1998) Role of citron kinase as a target of the small GTPase Rho in cytokinesis. *Nature*, **394**, 491–494.

Matsui,T. *et al*. (1996) Rho-associated kinase, a novel serine/threonine kinase, as a putative target for the small GTP binding protein Rho. *EMBO J.*, **15**, 2208–2216.

Miki,H., Sasaki,T., Takai,Y. and Takenawa,T. (1998) Induction of filopodium formation by a WASP-related actin-depolymerizing protein N-WASP. *Nature*, **391**, 93–96.

Olson,M.F., Ashworth,A. and Hall,A. (1995) An essential role for Rho, Rac and Cdc42 GTPases in cell cycle progression through G_1. *Science*, **269**, 1270–1272.

Paterson,H.F., Self,A.J., Garrett,M.D., Just,I., Aktories,K. and Hall,A. (1990) Microinjection of recombinant p21^{rho} induces rapid changes in cell morphology. *J. Cell Biol.*, **111**, 1001–1007.

Piacentini,M., Martinet,N., Beninati,S. and Folk,J.E. (1988) Free and protein-conjugated polyamines in mouse epidermal cells. Effect of high calcium and retinoic acid. *J. Biol. Chem.*, **263**, 3790–3794.

Reid,T., Furuyashiki,T., Ishizaki,T., Watanabe,G., Watanabe,N., Fujisawa,K., Morii,N., Madaule,P. and Narumiya,S. (1996) Rhotekin, a new putative target for Rho bearing homology to a serine/threonine kinase, PKN and rhophilin in the Rho-binding domain. *J. Biol. Chem.*, **271**, 13556–13560.

Schmidt,G., Sehr,P., Wilm,M., Selzer,J., Mann,M. and Aktories,K. (1997) Gln 63 of Rho is deamidated by *Escherichia coli* cytotoxic necrotizing factor-1. *Nature*, **387**, 725–729.

Schmidt,G., Selzer,J., Lerm,M. and Aktories,K. (1998) The Rho-deamidating cytotoxic necrotizing factor 1 from *Escherichia coli* possesses transglutaminase activity. *J. Biol. Chem.*, **273**, 13669–13674.

Sin,W., Chen,X., Leung,T. and Lim,L. (1998) RhoA-binding kinase α translocation is facilitated by the collapse of the vimentin intermediate filament network. *Mol. Cell. Biol.*, **18**, 6325–6339.

Takaishi,K., Sasaki,T., Kato,M., Yamochi,W., Kuroda,S., Nakamura,T., Takeichi,M. and Takai,Y. (1994) Involvement of Rho p21 small GTP-binding protein and its regulator in the HGF-induced cell motility. *Oncogene*, **9**, 273–279.

Uehata,M. *et al*. (1997) Calcium sensitization of smooth muscle mediated by a Rho-associated protein kinase in hypertension. *Nature*, **389**, 990–994.

von Eichel-Streiber,C., Boquet,P., Sauerborn,M. and Thelestam,M. (1996) Large clostridial cytotoxins—a family of glycosyltransferases modifying small GTP-binding proteins. *Trends Microbiol.*, **4**, 375–382.

Watanabe,G. *et al*. (1996) Protein kinase N (PKN) and PKN-related protein rhophilin as targets of small GTPase Rho. *Science*, **271**, 645–648.

Watanabe,N., Kato,T., Fujita,A., Ishizaki,T. and Narumiya,S. (1999) Cooperation between mDia1 and ROCK in Rho-induced actin reorganization. *Nature Cell Biol.*, **1**, 136–143.

Yamamoto,M., Marui,N., Sakai,T., Morii,N., Kozaki,S., Ikai,K., Imamura,S. and Narumiya,S. (1993) ADP-ribosylation of the *rhoA* gene product by botulinum C3 exoenzyme causes Swiss 3T3 cells to accumulate in the G_1 phase of the cell cycle. *Oncogene*, **8**, 1449–1455.

Zong,H., Raman,N., Mickelson-Young,L.A., Atkinson,S.J. and Quilliam,L.A. (1999) Loop 6 of RhoA confers specificity for effector binding, stress fiber formation and cellular transformation. *J. Biol. Chem.*, **274**, 4551–4560.